

Wright State University

CORE Scholar

Physics Faculty Publications

Physics

2-1-1989

A New Technique for Whole-Wafer Etch-Pit Density Mapping in GaAs

David C. Look

Wright State University - Main Campus, david.look@wright.edu

D. C. Walters

J. S. Sewell

S. C. Dudley

M. G. Mier

See next page for additional authors

Follow this and additional works at: <https://corescholar.libraries.wright.edu/physics>

 Part of the [Physics Commons](#)

Repository Citation

Look, D. C., Walters, D. C., Sewell, J. S., Dudley, S. C., Mier, M. G., & Sizelove, J. S. (1989). A New Technique for Whole-Wafer Etch-Pit Density Mapping in GaAs. *Journal of Applied Physics*, 65 (3), 1375-1377.
<https://corescholar.libraries.wright.edu/physics/112>

This Article is brought to you for free and open access by the Physics at CORE Scholar. It has been accepted for inclusion in Physics Faculty Publications by an authorized administrator of CORE Scholar. For more information, please contact library-corescholar@wright.edu.

Authors

David C. Look, D. C. Walters, J. S. Sewell, S. C. Dudley, M. G. Mier, and J. S. Sizelove

A new technique for whole-wafer etch-pit density mapping in GaAs

D. C. Look and D. C. Walters

University Research Center, Wright State University, Dayton, Ohio 45435

J. S. Sewell, S. C. Dudley, M. G. Mier, and J. S. Sixelove

Air Force Avionics Laboratory, AFWAL/AADR, Wright-Patterson Air Force Base, Ohio 45433

(Received 15 August 1988; accepted for publication 14 October 1988)

The pits formed on an etched GaAs surface, due to the anisotropic etching around dislocations, are efficient light scatterers, and thus reduce transmission. We have derived a quantitative relationship between the fractional transmission and the etch-pit density (EPD) and have shown that the same absorption apparatus which is commonly used to obtain a whole-wafer [EL2] map can also be used to generate an EPD map. The technique is verified by comparing the fractional transmission with the actual EPD count at 166 points on a three-inch, low-pressure, liquid-encapsulated Czochralski wafer. Also, [EL2] and EPD maps, with more than 3500 points each, are compared.

Semiconductor and device characterization have recently become more sophisticated because of the advent of computer-controlled stepping systems which allow large numbers of material parameters, such as the EL2 density, or device parameters, such as the pinch-off voltage of a field-effect transistor (FET), to be measured on a single wafer. Thus, it is often possible to "map" these parameters in a dense enough manner that variations due to crystal symmetry or processing problems can be readily seen, and meaningful correlations among the various parameters drawn.¹ However, up until now, there has been no convenient way to obtain whole-wafer data on dislocation density, because manual etch-pit density (EPD) counts, the standard method to determine the dislocation density, are slow and tedious, and highly dependent on operator experience. Recently, Dobrilla and Blakemore² suggested that a transmission experiment on an etched wafer, with 1.45- μm light, could give etch-pit information because light of that wavelength would be scattered by the etch pits but would not be strongly absorbed by EL2 or any other known defect or impurity which was likely to exist in semi-insulating (SI) GaAs. However, although Dobrilla and Blakemore obtained transmission maps related to the EPD, they did not quantify the relationship between transmission and EPD, and thus could not necessarily draw valid correlations with other parameters. We have derived a quantitative relationship, used it to calibrate the transmission maps of several etched, three-inch, SI GaAs wafers in various boules, and then statistically compared these maps with EL2 and device-parameter maps from nearby wafers in the same boules. A full report will be presented elsewhere, but here we simply describe and verify the technique, and show the relationship between EPD and EL2 for one particular wafer.

The wafers used for this study were grown by a low-pressure, liquid-encapsulated Czochralski technique. Five sequential wafers, Nos. 14–18, were processed at one particular device house, at which [EL2] measurements were also made, and five other wafers, Nos. 20–24, were processed at another device house. (It should be noted that comparative EL2 studies between our laboratory and the first device house yield nearly identical results.) Wafer No. 19, retained

by us, was etched in molten KOH at 450 °C for 40 min in a zirconium crucible. The fractional transmission, at 1.45 μm , was then measured in an apparatus which is shown schematically in Fig. 1. This same apparatus is also used to produce [EL2] maps, by using unetched wafers and a different wavelength (1.1 μm). The choice of 1.45- μm light for the EPD experiment is based upon two considerations: (1) the EL2 absorption is very weak at this wavelength, and (2) the detector sensitivity is very high. However, we have also successfully used 1.8- μm light, at which the EL2 absorption is even weaker.

The relationship between transmission and EPD is complicated by the fact that the etch pits can overlap, especially if the pits are large and their density is high. Let A_T be the total illuminated-spot size, and let A_E be the area within this spot size covered by etch pits. Now suppose we add dn etch pits of average area a . Then the increase in A_E , i.e., dA_E , is just $a dn (1 - A_E/A_T)$, to take account of the fact that some of the new etch pits will fall on areas already covered. Thus, if we define the EPD on a single surface as $\rho_D \equiv n/A_T$, the resulting differential equation yields the result A_E/A_T

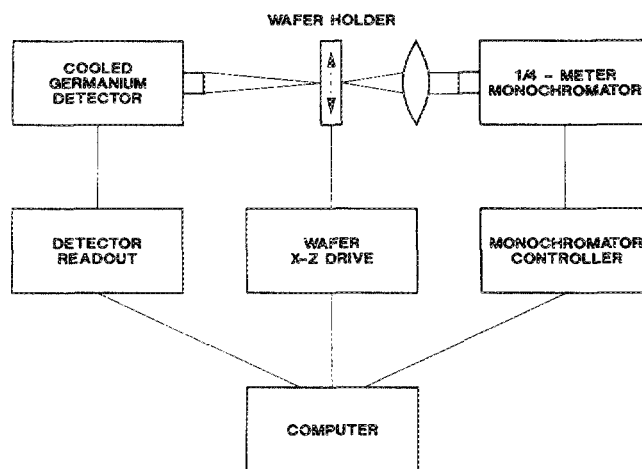


FIG. 1. An automated absorption apparatus useful for both [EL2] and EPD mapping.

$= [1 - \exp(-\alpha \rho_D)]$. A similar equation, in a somewhat different context, was derived by Rees, Stirland, and Bicknell.³

The fraction of light scattered by area A_E can be defined as $S \equiv \beta A_E / A_T = \beta [1 - \exp(-\alpha \rho_D)]$, where the parameter β can range from 0 to 1, depending on the scattering strength of the etch pits. Now since two etched surfaces are involved in this problem, multiple scatterings and reflections must be considered. By applying a summation technique, similar to that used to derive the classical transmission formula,⁴ it can be shown that

$$T = \frac{(1 - R)^2 (1 - S)^2 e^{-\alpha d}}{1 - R^2 (1 - S)^2 e^{-2\alpha d}}, \quad (1)$$

where α is the absorption coefficient, d the sample thickness, and R the reflectivity. In general, $R^2 (1 - S)^2 \ll 1$, and we always choose a wavelength such that $\alpha \approx 0$. Finally, we replace the unknown parameters R and β by more convenient parameters T_0 and T_E , where $T_0 = T(\alpha \rho_D \ll 1)$, and $T_E = T(\alpha \rho_D \gg 1)$. Then, Eq. (1) can be shown to yield

$$T^{1/2} = T_E^{1/2} + (T_0^{1/2} - T_E^{1/2}) e^{-\alpha \rho_D}. \quad (2)$$

For wafers which have both very high ($\rho_D a \gg 1$) and very low ($\rho_D a \ll 1$) etch-pit density regions, T_0 is simply the maximum, and T_E the minimum measured transmission. However, in general, it is probably better to carry out an actual etch-pit count at two points, 1 and 2. Then, T_0 and T_E can be related to the actual counts (ρ_{D1} and ρ_{D2}) and the fractional transmissions (T_1 and T_2) at these two points:

$$T_0^{1/2} = \frac{T_2^{1/2} (1 - e^{-\alpha \rho_{D1}}) - T_1^{1/2} (1 - e^{-\alpha \rho_{D2}})}{e^{-\alpha \rho_{D2}} - e^{-\alpha \rho_{D1}}}, \quad (3)$$

$$T_E^{1/2} = \frac{T_1^{1/2} e^{-\alpha \rho_{D2}} - T_2^{1/2} e^{-\alpha \rho_{D1}}}{e^{-\alpha \rho_{D2}} - e^{-\alpha \rho_{D1}}}. \quad (4)$$

With these values of T_0 and T_E , the transmission data can be converted directly to etch-pit data by inverting Eq. (2):

$$\rho_D = -\frac{1}{a} \ln \frac{T^{1/2} - T_E^{1/2}}{T_0^{1/2} - T_E^{1/2}}. \quad (5)$$

For this study, T_0 and T_E were obtained by picking points 1 and 2 at the center of the wafer, and halfway

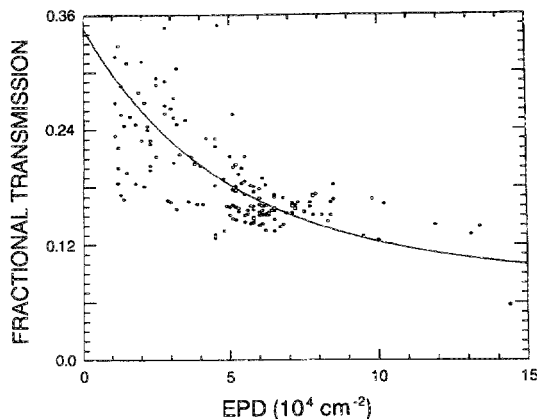


FIG. 2. The experimental (points) and theoretical (solid line) relationship of fractional transmission and actual etch-pit density.

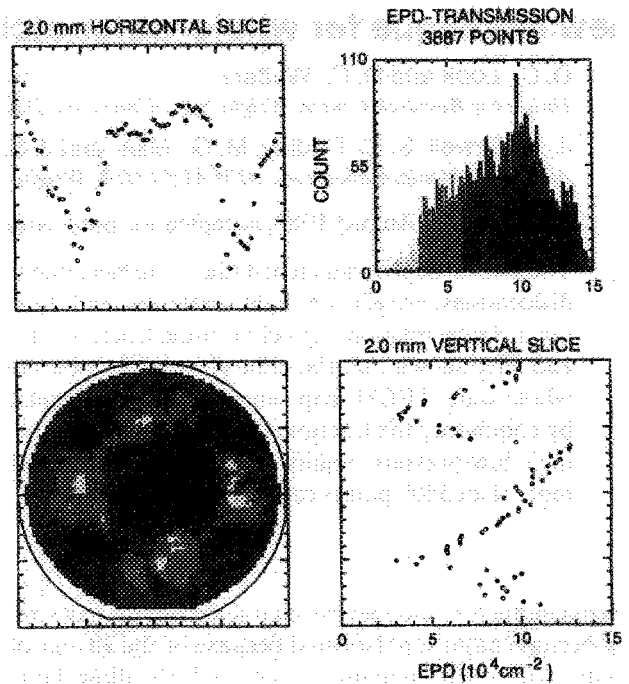


FIG. 3. The EPD map for a 3-in., low-pressure, LEC GaAs wafer (no. 19) obtained from transmission data which were converted via Eq. 5.

between the center and the top of the wafer, respectively. The average etch-pit size was measured to be $a = 1.5 \times 10^{-5}$ cm². The plot of Eq. (2), with these three parameters, is shown in Fig. 2. Also shown are 164 other manually counted points taken along horizontal, vertical, and diagonal lines through the center of the wafer. Although the scatter is seen to be high at low EPD values, the points clearly follow the

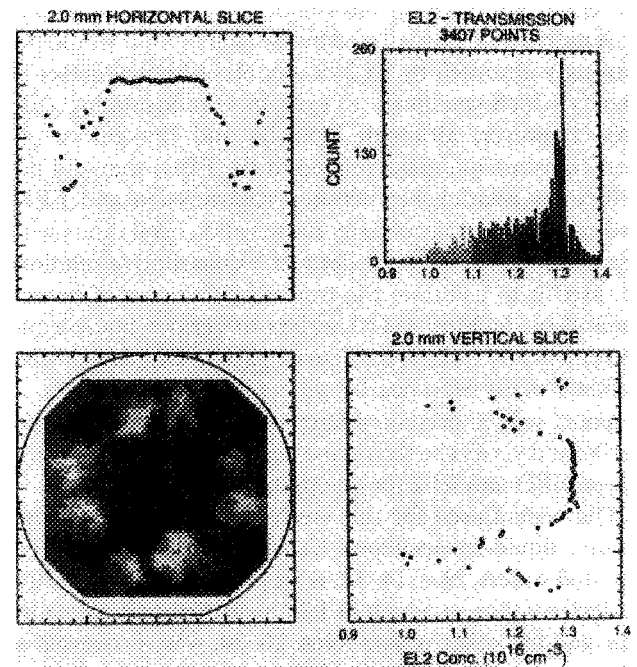


FIG. 4. The [EL2] map on wafer no. 18, obtained from 1.1- μ m transmission data at another laboratory.

theoretical line. Most of the scatter was due to inaccuracies in the manual-counting method, as was confirmed by repeatability studies. By using the calibration formula, Eq. (5), on all the points, the total EPD map could be generated and is shown in Fig. 3, along with a histogram and 2-mm horizontal [011] and vertical [0 $\bar{1}1$] data slices. The expected four-fold symmetry is clearly seen in these data. For comparison, in Fig. 4 we show an [EL2] map, taken on adjacent wafer No. 18 by personnel at another laboratory.⁵ The principal features are very similar, since both are strongly influenced by stress appearing during crystal growth.⁶ Comparisons with FET parameters, from wafers 20 and 21, and repeatability studies for both the manual and automated EPD techniques, will be published elsewhere.

In summary, we have developed an experimental and theoretical method for obtaining whole-wafer etch-pit density (dislocation) maps. The apparatus is quite simple, and is already in use for [EL2] measurements. It is now possible to

obtain both dense [EL2] and dense EPD data to statistically compare with the dense device-parameter data available from automated wafer probers.

We wish to thank S. Brierley, of Raytheon, Inc., for the EL2 data shown in Fig. 4. Also, we are grateful to B. Johnson for technical assistance, and to J. King and R. T. Kemerley for helpful discussions. The work of D. Look and D. Walters was supported by the U.S. Air Force under Contract No. F33615-86-C-1062.

¹P. Dobrilla, J. S. Blakemore, A. J. McCamant, K. R. Gleason, and R. Y. Koyama, *Appl. Phys. Lett.* **47**, 602 (1985).

²P. Dobrilla and J. S. Blakemore, *J. Appl. Phys.* **60**, 169 (1986).

³G. J. Rees, D. J. Stirling, and R. W. Bicknell, *Mater. Lett.* **4**, 455 (1986).

⁴J. I. Pankove, *Optical Processes in Semiconductors* (Dover, New York, 1971), p. 93.

⁵Raytheon, Inc., 131 Spring St., Lexington, MA, 02173.

⁶D. E. Holmes, R. T. Chen, K. R. Elliott, and C. G. Kirkpatrick, *Appl. Phys. Lett.* **43**, 305 (1983).

Observation of interface defects in strained InGaAs-GaAs by photoluminescence spectroscopy

M. J. Joyce

Telecom Australia Research Laboratories, 770 Blackburn Road, Clayton, Victoria 3168, Australia

M. Gal and J. Tann

School of Physics, University of New South Wales, P.O. Box 1, Kensington, NSW 2033, Australia

(Received 11 May 1988; accepted for publication 29 September 1988)

We have described a number of new, broad-linewidth emission bands in the photoluminescence spectrum of strained InGaAs-GaAs single-quantum wells. The variation of the luminescence intensity as a function of layer thickness and excitation intensity suggests that these bands are caused by interface defects, most likely misfit dislocations at the InGaAs/GaAs interface.

Recently much attention has been given to strained single-quantum wells (SSQW) and strained-layer superlattices (SLS).¹⁻³ Strained-layer heterostructures allow the use of lattice-mismatched alloys, such as InGaAs and GaAs, with layer thickness small enough to accommodate the lattice strain coherently rather than by misfit dislocations. As the layer thickness increases above a certain composition-dependent critical value, the strain is relaxed by the generation of misfit dislocations. In this communication, we report the observation of new very broad-linewidth photoluminescent emission bands which we believe are caused by misfit dislocations at the GaAs/InGaAs interface.

Previously we have reported photoluminescence (PL) from the band gap (excitons or confined particles) of InGaAs/GaAs SSQW⁴ and single heterostructures⁵ of various In mole fraction and we have deduced the variation of strain in the InGaAs with layer thickness. The SSQWs and heterostructures exhibited extremely narrow luminescence linewidths⁴ and high luminescence efficiency confirming their excellent crystalline quality. In fact, the linewidth for the narrowest (fully strained) layers was close to the theo-

retical limit set by compositional fluctuations and temperature.⁶ In this communication, we report the observation of a number of broad luminescent bands in the low-temperature PL spectra of high-quality In_{0.17}Ga_{0.83}As-GaAs SSQWs. These emission bands were studied as a function of InGaAs layer thickness as well as the GaAs capping layer thickness. The results suggest that the bands are caused by misfit dislocations that are generated at the GaAs/InGaAs interface.

Dislocations in this family of materials have been directly observed by photoluminescence microscopy by Gourley *et al.*^{7,8} They have shown that the PL intensity is reduced in the proximity of dislocations thus allowing their microscopic observation. Here we show that in addition to reducing the PL intensity, dislocations also introduce additional states in the band gap of InGaAs that are detectable by PL spectroscopy.

The MBE-grown GaAs/In_{0.17}Ga_{0.83}As/GaAs single-quantum wells (or double heterostructures) consist of a 3000-Å-thick GaAs buffer layer grown on semi-insulating GaAs:Cr followed by an undoped In_{0.17}Ga_{0.83}As layer of thickness h , where $100 \text{ Å} < h < 10\,000 \text{ Å}$. The InGaAs layer